# Bcl11b is essential for group 2 innate lymphoid cell development

Jennifer A. Walker,[1] Christopher J. Oliphant,[1] Alexandros Englezakis,[1] Yong Yu,[2] Simon Clare,[2] Hans-Reimer Rodewald,[3] Gabrielle Belz,[4,5] Pentao Liu,[2] Padraic G. Fallon,[6,7,8] and Andrew N.J. McKenzie[1]

[1]Medical Research Council (MRC) Laboratory of Molecular Biology, Cambridge CB2 0QH, England, UK
[2]Wellcome Trust Sanger Institute, Hinxton, Cambridge CB10 1HH, England, UK
[3]Division of Cellular Immunology, German Cancer Research Center, 69120 Heidelberg, Germany
[4]The Walter and Eliza Hall Institute of Medical Research, Parkville, Melbourne, Victoria 3052, Australia
[5]Department of Medical Biology, University of Melbourne, Melbourne, Victoria 3010, Australia
[6]Trinity Biomedical Sciences Institute and [7]Institute of Molecular Medicine, Trinity College Dublin, Dublin 2, Ireland
[8]National Children's Research Centre, Our Lady's Children's Hospital, Crumlin, Dublin 12, Ireland

Group 2 innate lymphoid cells (ILC2s) are often found associated with mucosal surfaces where they contribute to protective immunity, inappropriate allergic responses, and tissue repair. Although we know they develop from a common lymphoid progenitor in the bone marrow (BM), the specific lineage path and transcriptional regulators that are involved are only starting to emerge. After ILC2 gene expression analysis we investigated the role of Bcl11b, a factor previously linked to T cell commitment, in ILC2 development. Using combined Bcl11b–tom and Id2–gfp reporter mice, we show that *Bcl11b* is expressed in ILC2 precursors in the BM and maintained in mature ILC2s. In vivo deletion of *Bcl11b*, by conditional tamoxifen–induced depletion or by *Bcl11b*$^{-/-}$ fetal liver chimera reconstitution, demonstrates that ILC2s are wholly dependent on Bcl11b for their development. Notably, in the absence of Bcl11b there is a concomitant expansion of the RORγt$^+$ ILC3 population, suggesting that Bcl11b may negatively regulate this lineage. Using *Nippostrongylus brasiliensis* infection, we reveal that the absence of Bcl11b leads to impaired worm expulsion, caused by a deficit in ILC2s, whereas *Citrobacter rodentium* infection is cleared efficiently. These data clearly establish Bcl11b as a new factor in the differentiation of ILC2s.

CORRESPONDENCE
Jennifer A. Walker:
jwalker@mrc-lmb.cam.ac.uk
OR
Andrew N.J. McKenzie:
anm@mrc-lmb.cam.ac.uk

Abbreviations used: CHILP, common helper ILC progenitor; FL, fetal liver; ILC, innate lymphoid cell; ILC2p, ILC2 precursor; MLN, mesenteric LN; NKp, NK-like precursor; p.i., postinfection; PLZF, promyelocytic leukemia zinc finger; siLP, small intestine lamina propria.

The recently identified innate lymphoid cell (ILC) family consists of IFN-γ–secreting group 1 ILCs (ILC1s), type 2 cytokine-producing ILC2s, and IL-22– and/or IL-17–positive ILC3s (Walker et al., 2013). ILC1s and ILC3s play critical roles in protective immunity against bacteria, intracellular protozoan parasites (ILC1), and fungi (ILC3) and in autoimmune disorders (McKenzie et al., 2014). In contrast, ILC2s associate with immune responses to parasitic worms, allergy, and wound repair (McKenzie et al., 2014).

These functionally diverse cytokine-producing cells arise from a common lymphoid progenitor under the control of specific transcriptional regulators (Diefenbach et al., 2014). These include upstream factors such as inhibitor of DNA binding 2 (Id2), Notch, GATA-binding protein 3 (GATA3), nuclear factor

interleukin-3 (Nfil3), T cell factor 1 (TCF1), and promyelocytic leukemia zinc finger (PLZF) that restrict the differentiation of a common helper ILC progenitor (CHILP) from the common lymphoid progenitor (Diefenbach et al., 2014). Downstream, lineage-specific transcription factors are necessary for lineage commitment: ILC1s require the T-box transcription factor T-bet (*Tbx21*), ILC2s require GATA3 and transcription factor retinoic acid receptor–related orphan nuclear receptor α (RORα), and ILC3s require RORγt (Diefenbach et al., 2014). Notably, the majority of factors identified in these pathways play roles in the specification of the progenitor cells and lie proximal to the division of the functional ILC subsets.

The Rockefeller University Press $30.00
J. Exp. Med. 2015 Vol. 212 No. 6 875–882
www.jem.org/cgi/doi/10.1084/jem.20142224

875

Although they comprise only a small proportion of the hematopoietic compartment, ILC2s (often at the mucosal borders) are a critical innate cellular source of type 2 cytokines, secreting copious IL-5 and IL-13, but also IL-9, IL-4, and GM-CSF (Moro et al., 2010; Neill et al., 2010; Price et al., 2010). These effector cytokines potently induce eosinophilia, goblet cell hyperplasia and mucus production, mastocytosis, alternatively activated macrophages, and muscle contractility and contribute to tissue repair (McKenzie et al., 2014). Thus, ILC2s that expand in response to the type 2 initiator cytokines IL-25, IL-33, and TSLP play a key role in protective immunity against parasitic helminth infection (Moro et al., 2010; Neill et al., 2010; Price et al., 2010), contribute to inappropriate allergic inflammation (Barlow et al., 2011; Chang et al., 2011; Mjösberg et al., 2011), and are associated with metabolic homeostasis, obesity, and dietary stress (Hams et al., 2013; Molofsky et al., 2013; Stanya et al., 2013).

ILC2s can be derived from a PLZF$^+$ fraction of CHILPs, and conditional deletion of GATA3 in Id2$^+$ cells or germline deletion has demonstrated that GATA3 is required both for the development of all ILCs and for the later restriction of the ILC2 lineage (Hoyler et al., 2012; Yagi et al., 2014). In contrast, RORα–deficient mice have apparently normal CHILP and ILC3 production, but BM progenitors from these mice fail to develop into ILC2s, both in vivo and in vitro (Halim et al., 2012; Wong et al., 2012). In addition to RORα and GATA3, the transcription factor B cell leukemia/lymphoma 11b (Bcl11b) was also reported to be up–regulated in ILC2s, but its role remained undefined (Wong et al., 2012). Bcl11b is a zinc finger transcription factor that is required at multiple developmental checkpoints for T cell commitment and maintenance (Avram and Califano, 2014). Germline deletion of *Bcl11b* results in homozygous mice dying shortly after birth from a complex idiopathic disease, and although hematopoiesis appears normal, there is a block in thymocyte development at the double–negative 2 (DN2) stage (Wakabayashi et al., 2003). These Bcl11b-deficient DN2 thymocytes were highly proliferative in vivo, and although they could not develop into T cells, they retained the potential to differentiate into NK cells and myeloid lineages. Interestingly, conditional depletion of *Bcl11b* resulted in T cells acquiring an NK cell–like phenotype, indicating that Bcl11b is crucial for maintaining T cell commitment and repressing alternative lineage choices (Li et al., 2010b). Given the critical role of Bcl11b in T lymphocyte development and its elevated expression in ILC2s, we investigated the role of Bcl11b in ILC2 development and function.

## RESULTS AND DISCUSSION
### Bcl11b is expressed in ILC2 precursors and throughout ILC2 development

To assess the expression of Bcl11b in ILC2 populations, we used a Bcl11b-tdtomato (Bcl11b-tom) knock-in mouse (*Bcl11b$^{tom/+}$*) in which Bcl11b-tom expression acts as a surrogate for *Bcl11b* expression (Li et al., 2010b). CD4$^+$ (Fig. 1 a) and CD8$^+$ T cells (not depicted) from the mesenteric LNs (MLNs) were strongly positive for Bcl11b-tom, whereas B cells

and myeloid cells were negative (not depicted). ILC2s (phenotypic analysis and gating strategies in Figs. S1 and S2), isolated from ILC2-associated immunological sites in naive mice, also expressed Bcl11b-tom similar to T cells (Fig. 1, a–c). Bcl11b-tom expression was reduced slightly in ILC2s after in vivo stimulation with IL-25 and IL-33 (Fig. 1, c and d); the reason for this is unclear. Thus, mature ILC2s express high amounts of *Bcl11b* in the peripheral lymphoid tissues. Bcl11b-tom expression was also detected in ILC2-like cells in the BM, suggesting that it may be present in ILC2 precursors (ILC2ps; Fig. 1 e). Notably, Bcl11b-tom was also expressed heterogeneously in a proportion of non-LTi ILC3s from the small intestine lamina propria (siLP; Fig. 1 f and Fig. S2 a).

### Characterization of a Bcl11b–expressing ILC2ps

Because mature ILC2s arise from ILC2ps in the BM, we sought to identify whether ILC2ps express Bcl11b. We identified BM-derived ILC2ps (ICOS$^+$) using mice in which *Id2* expression, which marks early NK progenitors (Carotta et al., 2011) and is required for the development of all ILC subsets, is reported by the expression of an IRES green fluorescent protein (*Id2$^{gfp/+}$*; Jackson et al., 2011), in combination with surface markers to exclude NK-like precursors (NKps; CD244). Thus, the lin$^-$Id2-gfp$^+$ BM cell population was subdivided by ICOS and/or CD244 into four subsets (Fig. S2 b). To assess their lineage commitment, these cells were purified and plated onto OP9 or OP9–Delta-like ligand 1 (DL1) cell monolayers in the presence of ILC2-promoting IL-7 and IL-33 or NK-promoting IL-7 and IL-15. We demarcated ILC2ps (lin$^-$Id2-gfp$^+$ICOS$^+$CD244$^-$; Fig. 2, a and c) and NKps (lin$^-$Id2-gfp$^+$ICOS$^-$CD244$^+$; Fig. 2, b and c). In some instances, cultures gave rise to additional populations of cells (CD3$^-$, CD19$^-$, CD11b$^-$, CD11c$^-$, Gr-1$^-$, NK1.1$^-$, NKp46$^-$) that could not be ascribed to any particular lineage. Subsequent analysis of intercrossed *Id2$^{gfp/+}$* and *Bcl11b$^{tom/+}$* mice demonstrated that expression of Bcl11b-tom was almost mutually exclusive in the ILC2p and NKp populations, being expressed only by the ILC2ps, both upon direct isolation from the BM and after culture on OP9-DL1 feeder cells to produce ILC2s (Fig. 2, d and e).

To confirm the progenitor status of the Bcl11b$^+$ BM cells, we isolated Id2-gfp$^+$Bcl11b$^+$ICOS$^+$ or Id2-gfp$^+$Bcl11b$^-$CD244$^+$ BM precursor subsets and transferred these into *Rag2$^{-/-}$γc$^{-/-}$* recipient mice (Fig. S2, c and d). Only Id2-gfp$^+$Bcl11b$^+$ precursors gave rise to ILC2s upon adoptive transfer (Fig. 2 f). Transfer of the Id2-gfp$^+$Bcl11b$^-$ precursors gave rise to NK cells (Fig. 2 g). Comparison of the Id2-gfp$^+$Bcl11b$^+$ precursors with the previously reported Lin$^-$Sca1$^{hi}$Id2$^{hi}$ (LSI) precursor (Fig. S2, e and f; Hoyler et al., 2012) indicated that they are very similar (Fig. 2 h) and give rise to phenotypically identical Gata3$^+$KLRG1$^+$ ILC2s upon adoptive transfer into *Rag2$^{-/-}$γc$^{-/-}$* recipients (Fig. 2, i and j). These transfers also generated a population of Gata3$^-$ICOS$^+$KLRG1$^-$ cells, the significance of which is unclear, but that may represent immature ILC2s (Fig. 2, i and j).
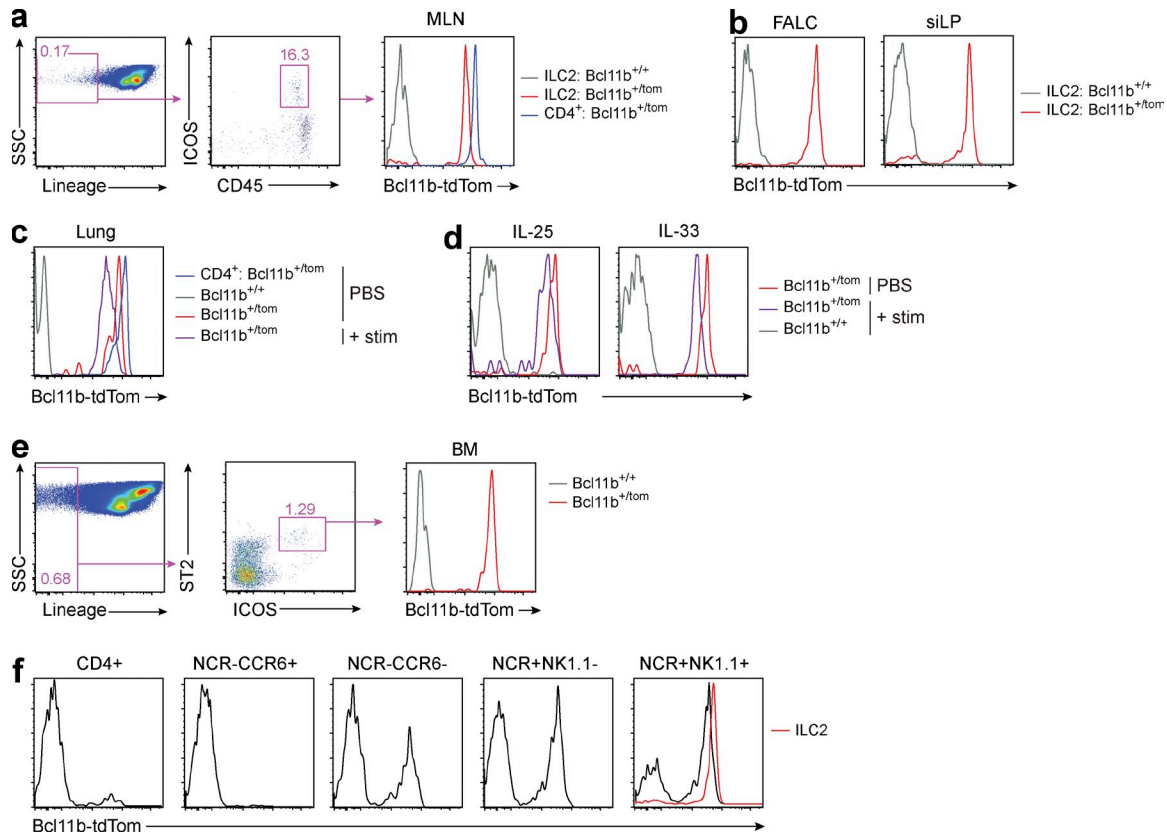
**Figure 1. Bcl11b is expressed throughout the ILC2 lineage.** (a–f) Bcl11b-tom in cells isolated from Bcl11b^tom/+ mice, assessed by flow cytometry. (a and b) Bcl11b-tom expression in ILC2s and CD4+ T cells from the MLN (a) and ILC2s from FALC (lin−CD45+KLRG1+) and siLP (lin−CD45+ICOS+KLRG1+; b) of Bcl11b+/+ and Bcl11b^tom/+ mice. (c and d) Bcl11b-tom expression in ILC2s from lung (c) and MLN (d) of mice with the indicated genotypes after administration of IL-25 or IL-33. (e) Expression of Bcl11b-tom in BM ILC2ps (gated as shown). (f) Bcl11b-tom expression in ILC3 subsets (as indicated) from siLP of Bcl11b^tom/+ mice (black). Bcl11b-tom expression in ILC2s from siLP is shown for comparison (red). (a–f) Numbers adjacent to boxed areas indicate the relative percentage of gated populations. Gating strategies and phenotypic analysis are presented in Figs. S1 and S2. Data represent at least two independent experiments with three mice per group.

Although the majority of ICOS+CD244+ cells were *Bcl11b−*, ICOS−CD244− cells displayed bimodal expression of Bcl11b-tom (Fig. 2 k). Upon culture under ILC2- or NK-promoting conditions, the Bcl11b+ fraction gave rise exclusively to ILC2s, whereas the Bcl11b− subset gave rise to mixed progeny (Fig. 2, l and m), suggesting that they may represent a mixed population of uncommitted precursors. Finally, we examined the expression of Gata3 in populations delineated by Id2-gfp and Bcl11b-tom and found that Gata3 is up-regulated in Id2-expressing cells, perhaps before the induction of Bcl11b (Fig. 2 n). These results demonstrate that Bcl11b is expressed by a lineage-restricted ILC2p and that, in combination with Id2, expression of Bcl11b can be used to purify the ILC2ps.

### Deletion of Bcl11b ablates ILC2s and increases ILC3s

We next sought to determine whether Bcl11b was functionally important for ILC2 development or maintenance. Tamoxifen was used to delete Bcl11b in conditional Bcl11b-deficient (*Cre-ERT2; Bcl11b^flox/flox*) mice (Li et al., 2010b), and ILC2 frequency was analyzed 2 wk later. Relative to

controls, tamoxifen treatment did not alter ILC2 numbers in the MLNs (Fig. 3 a and Fig. S3 a), although we did observe a reduction in the relative frequency of ILC2s (Fig. S3 a), which may reflect as yet not understood changes in multiple cell populations. Bcl11b deletion did not affect the frequency of BM ILC2p (Fig. 3 b) or Gata3 expression (Fig. 3 c). We next examined the effect of Bcl11b depletion in the context of ILC2 stimulation by IL-33. Conditional Bcl11b-deficient (*Bcl11b^flox/−*) mice bearing an Id2-gfp allele, intercrossed with *Rosa26Cre-ERT2* mice (*Cre-ERT2; Bcl11b^flox/−* referred to hereafter as *Bcl11b^flox/−*), *Bcl11b^flox/−* mice, or controls (*Cre-ERT2; Bcl11b^+/−* referred to hereafter as *Bcl11b^+/−*) were treated with tamoxifen. After IL-33 stimulation, there were considerably fewer ILC2s in the MLNs of the *Bcl11b^flox/−* mice as compared with the *Bcl11b^+/−* controls, which did not reach statistical significance but was consistent between two similar experiments (Fig. 3 d and Fig. S3 b). Tamoxifen administration was accompanied by a fall in the numbers of T cells in the absence of Bcl11b (Fig. 3 e) and a reciprocal increase in NK1.1+ cell numbers (Fig. 3 f), as reported previously (Li et al., 2010b). These findings suggest that Bcl11b is not required for
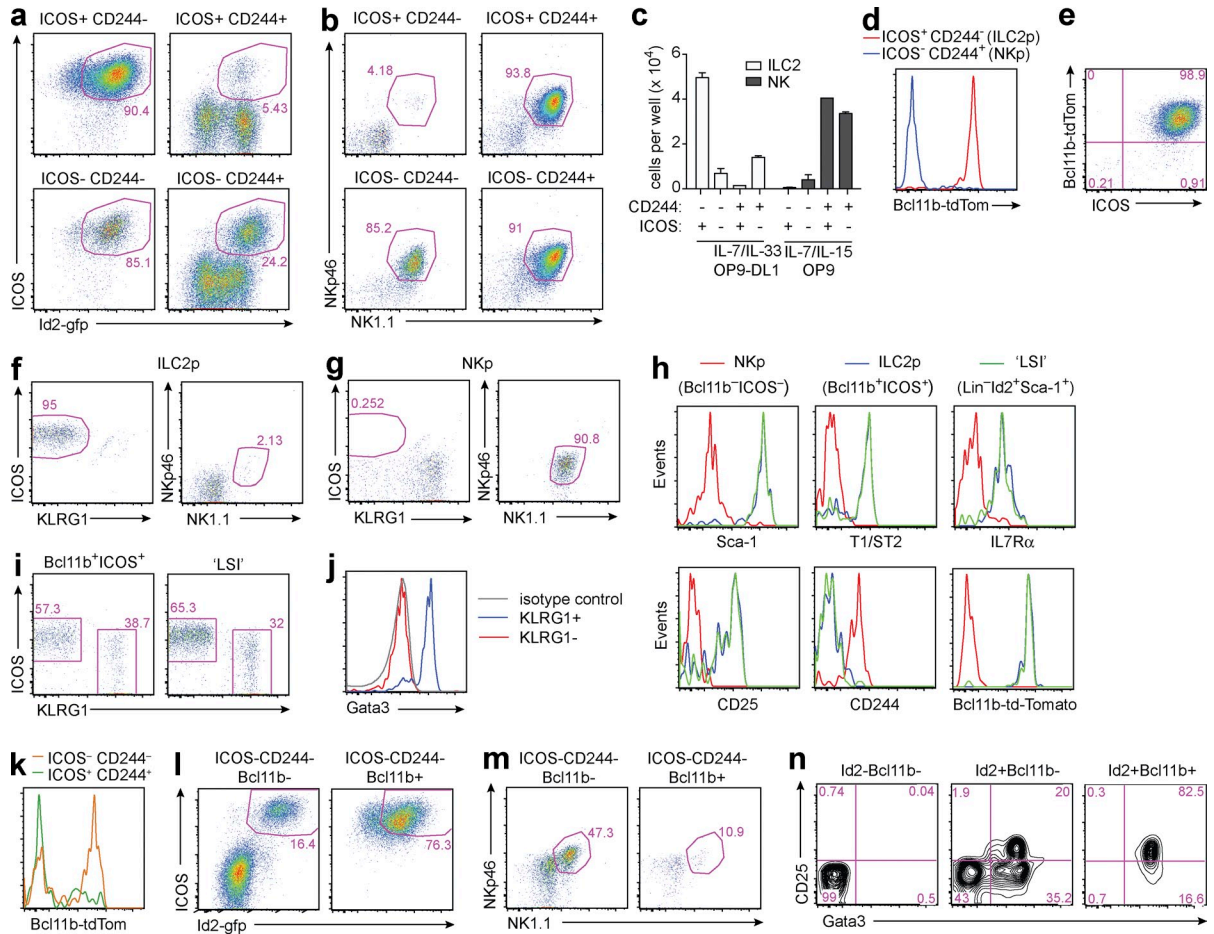
**Figure 2. Bcl11b expression defines ILC2ps in the BM.** (a–n) ICOS⁺CD244⁻ (ILC2p), ICOS⁺CD244⁺, ICOS⁻CD244⁺ (NKp), and ICOS⁻CD244⁻ subsets were isolated from lin⁻Id2-gfp⁺ BM cells and cultured in vitro (a–c, e, l, and m) or adoptively transferred into alymphoid recipients (f, g, i, and j) to assess their lineage potential; flow cytometry of lin⁻Id2-gfp⁺ subsets (d, h, k, and n) is shown. (a and b) The phenotype of the indicated cell populations cultured for 11 d on OP9-DL1 stromal cells in the presence of IL-7 and IL-33 (a) or cultured for 11 d on OP9 stromal cells in the presence of IL-7 and IL-15 (b). (c) Cells (1,000 per well) were cultured for 11 d under the conditions indicated. Bar graph depicts the number of cells in the final culture represented by ILC2s (Id2-gfp⁺ICOS⁺) and NK cells (NKp46⁺NK1.1⁺). Shown are mean ± SEM pooled from two independent experiments with two to three technical replicates per group. (d) Bcl11b-tom expression in ILC2p (lin⁻Id2-gfp⁺ICOS⁺CD244⁻) and NKp (lin⁻Id2-gfp⁺ICOS⁻CD244⁺) cells. (e) Bcl11b-tom expression in ILC2ps after culture on OP9-DL1 stromal cells for 13 d in the presence of IL-7 and IL-33. (f and g) ILC2ps (f) and NKps (see Fig. S2 c for gating; g) were adoptively transferred into *Rag2⁻/⁻γc⁻/⁻* recipients (∼700 cells per recipient). Plots show flow cytometric analysis of progeny, identified by Id2-gfp⁺ expression (Fig. S2 d), from spleen at 3 wk after transfer. (h) Surface marker expression of NKp, ILC2p, and LSI progenitor cell populations, gated as indicated in Fig. S2 e. (i and j) Approximately 700 ILC2p (lin⁻Flt3⁻Id2-gfp⁺ICOS⁺Bcl11b⁺) or LSI (lin⁻Sca-1⁺Id2-gfp⁺) cells (see Fig. S2 f for gating) were adoptively transferred into *Rag2⁻/⁻γc⁻/⁻* recipients. Plots show flow cytometric analysis of progeny, identified by Id2-gfp⁺ expression, from siLP at 6 wk after transfer (i), and panel j shows intracellular Gata3 staining of progeny. (k) Bcl11b-tom expression in ICOS⁻CD244⁻ and ICOS⁺CD244⁺ subsets. (l and m) The phenotype of Bcl11b⁻ and Bcl11b⁺ fractions of the ICOS⁻CD244⁻ population, after culture for 11 d on OP9-DL1 stromal cells in the presence of IL-7 and IL-33 (l) or on OP9 stromal cells in the presence of IL-7 and IL-15 (m). (n) Intracellular Gata3 staining was assessed on lin⁻ BM cells, sorted as indicated. (d, h, and k) Data represent at least three independent experiments with at least three mice per group. (a–c, e, l, and m) Data represent two independent experiments with two to three technical replicates per group. (f, g, and i) Data represent two independent experiments with three mice per group. (j) Data represent a single experiment using cells pooled from three mice. (n) Data represent two independent experiments using cells pooled from three mice.

the short-term maintenance of ILC2s in tissues. However, they raise the question of whether Bcl11b is required for ILC2 expansion in the tissues or for the continued generation of ILC2ps in the BM.

To address this question and the potential issues of dosing and off-target effects of tamoxifen, we also generated fetal liver (FL) chimeras in which irradiated CD45.2⁺ hosts were reconstituted with CD45.1⁺ BM, in combination with either CD45.2⁺ *Bcl11b⁺/⁺Id2^{gfp/+}* or *Bcl11b⁻/⁻Id2^{gfp/+}* FL. After 6–8 wk, there was an absence of FL donor-derived double-positive thymocytes in mice receiving *Bcl11b⁻/⁻* FL (Fig. 3 g), but no significant difference in the numbers of FL donor-derived Id2-gfp⁺ NK cells (Fig. 3 g). Strikingly, there was a total absence of mature FL donor-derived Id2-gfp⁺ ILC2s from the

*Bcl11b$^{-/-}$* FL in the MLNs, as compared with wild type (Fig. 3 h and Fig. S3 c). Furthermore, *Bcl11b$^{-/-}$*-derived ILC2s could not be induced by treatment with IL-33 (Fig. 3 h and Fig. S3 c) or IL-25 (not depicted). There were also no detectable FL donor-derived Id2-gfp$^+$ ILC2ps in the BM (Fig. 3 i and Fig. S3 d). Notably, analysis of ILCs in the siLP and MLN showed that the *Bcl11b$^{-/-}$* donor cells gave rise to a disproportionately large population of NCR$^+$ ILC3s as compared with wild type (Fig. 3, j and k; and Fig. S3 e).

Thus, Bcl11b is essential for the development of ILC2ps and consequently mature peripheral ILC2s. The complete absence of ILC2s in these mice is striking because residual ILCs have been observed after deletion of many of the previously reported factors that are important for ILC development. Indeed, even in the absence of RORα a basal level of ILC2s can be detected in the peripheral tissues (Wong et al., 2012). This implies that Bcl11b may act upstream of RORα during ILC2 development, although genetic complementation systems would be required to confirm this relationship.

We noted that although the absence of Bcl11b resulted in the loss of ILC2s, its absence also caused a reciprocal increase in the numbers of ILC3s in the siLP. This suggests that Bcl11b may act cell-intrinsically to repress ILC3 differentiation and that deletion of Bcl11b results in de-repression of the ILC3 program, leading to their expansion, or that the absence of ILC2s results in an expansion of ILC3s through cell-extrinsic factors.

## Bcl11b–deficient progenitors fail to provide ILC2s during *Nippostrongylus brasiliensis* infection

ILC2s play critical roles in immunity to infection with parasitic helminths, such as *N. brasiliensis*. Consequently, mice deficient in the ILC2-inducing cytokines IL-25 and IL-33 (Neill et al., 2010) or the transcription factor RORα (Wong et al., 2012; Oliphant et al., 2014) have impaired worm clearance. To confirm that the deletion of Bcl11b resulted in the absence of functional ILC2s in vivo, and not for example a loss of specific lineage markers, we determined whether Bcl11b deletion in ILC2s impaired *N. brasiliensis* clearance. However, because T cells are important for maintaining ILC2s during the later stages of *N. brasiliensis* clearance (Wong et al., 2012; Oliphant et al., 2014) and the *Bcl11b$^{-/-}$* chimeric mice have impaired T cell responses, we used a mixed chimera approach. We determined whether *Bcl11b$^{+/+}$* or *Bcl11b$^{-/-}$* FL could complement for the absence of ILC2ps in the BM of ILC2-deficient mice infected with *N. brasiliensis*. The ILC2-deficient (*Rora$^{sg/flox}$Il7r$^{Cre/+}$*) mice delete *Rora* in the lymphoid lineage, resulting in a loss of ILC2s without perturbing other hematopoietic lineages, thereby ensuring the continued presence of T cells (Oliphant et al., 2014).

Irradiated recipients were reconstituted with combinations of BM obtained from *Rora$^{flox/+}$* or *Rora$^{sg/flox}$* mice carrying the *Il7r-Cre* allele (Schlenner et al., 2010) and *Bcl11b$^{+/+}$Id2$^{gfp/+}$*– or *Bcl11b$^{-/-}$Id2$^{gfp/+}$*-derived FL and infected with *N. brasiliensis*. Mice receiving the *Rora$^{flox/+}$Il7r$^{Cre/+}$* BM generated ILC2s
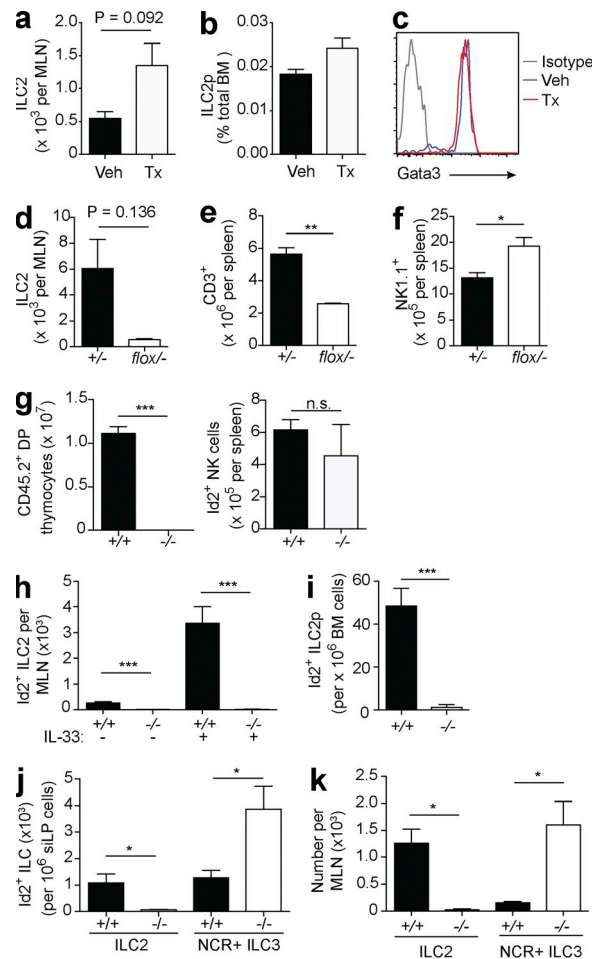


**Figure 3. ILC2s fail to develop in the absence of Bcl11b.** (a–k) Flow cytometry was performed to enumerate the indicated cell populations in conditional *Bcl11b*-deficient mice (a–f) or chimeras generated using *Bcl11b$^{-/-}$* FL cells (g–k). (a and b) MLN ILC2s (a) and BM ILC2ps (b) in *Cre-ERT2; Bcl11b$^{flox/flox}$* mice, treated as indicated (Veh, vehicle control; Tx, tamoxifen). Shown is mean ± SEM from two similar experiments with three to four mice per group. (c) Intracellular Gata3 staining in ILC2s from the MLNs of *Cre-ERT2; Bcl11b$^{flox/flox}$* mice, treated as indicated. (d–f) MLN ILC2 (d), splenic CD3$^+$ (e), and splenic NK1.1$^+$ cells (f) after the administration of tamoxifen and IL-33 (+/− = *Cre-ERT2; Bcl11b$^{+/-}$*; flox/− = *Cre-ERT2; Bcl11b$^{flox/-}$*). Mean ± SEM from two similar experiments with two to three mice per group. (g) The indicated cell populations were enumerated in mice 6–8 wk after reconstitution with either *Bcl11b$^{+/+}$* or *Bcl11b$^{-/-}$* CD45.2$^+$ FL, mixed with CD45.1$^+$ BM. Bars represent mean ± SEM of five mice per group. Data represent three independent experiments. (h) ILC2s (lin$^-$Id2-gfp$^+$ICOS$^+$KLRG1$^+$) in the MLN of mice reconstituted as in panel g, after PBS or IL-33 administration. (i–k) BM ILC2ps (lin$^-$Id2-gfp$^+$Sca-1$^+$ST2$^+$; i), siLP ILC2s (lin$^-$Id2-gfp$^+$KLRG1$^+$) and NCR$^+$ ILC3s (lin$^-$Id2-gfp$^+$NKp46$^+$; j) and MLN ILC2s and NCR$^+$ ILC3s (k) in mice reconstituted as in panel g; (h–j) mean ± SEM; (k) mean ± SD. P-values refer to Student's *t* test analysis: *, P < 0.05; **, P < 0.01; ***, P < 0.001.

(Fig. 4 a) and cleared the majority of their worms by day 7 postinfection (p.i.; Fig. 4 b). In contrast, mice receiving *Rora$^{sg/flox}$Il7r$^{Cre/+}$* BM failed to produce ILC2s or clear their worm burden by day 7 (Fig. 4, a and b). Reconstitution with
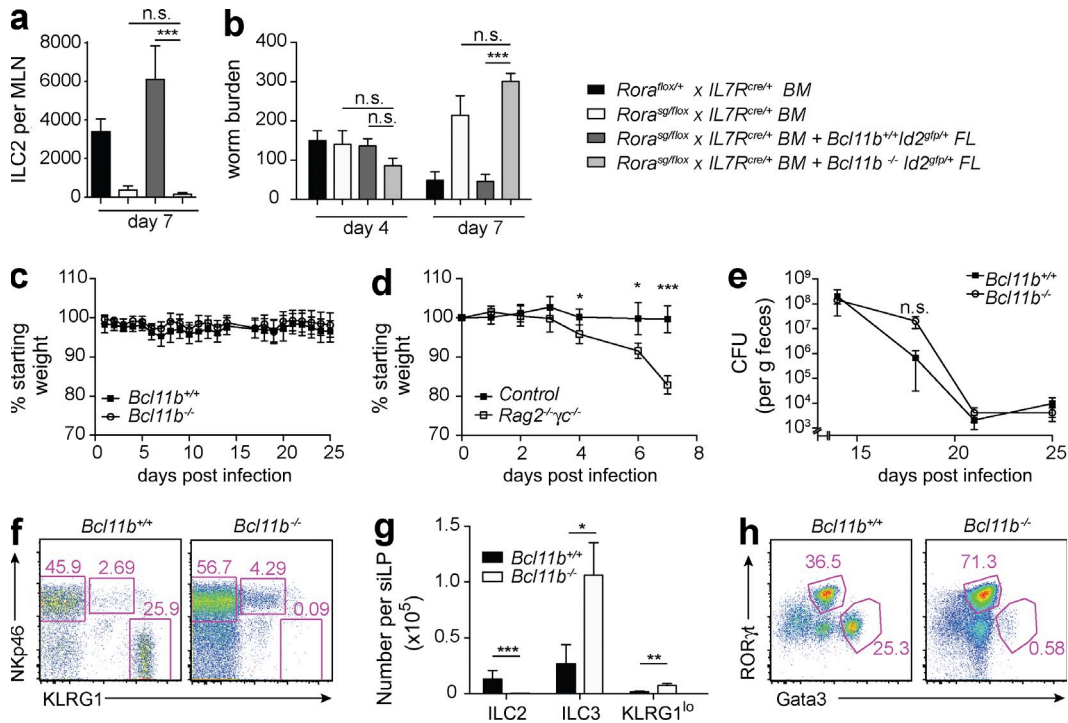
**Figure 4.** **Bcl11b is essential for clearance of *N. brasiliensis* infection but not clearance of *C. rodentium*.** (a–h) *Bcl11b*-deficient FL cells were used to generate chimeric mice that were either partially (ILC2s only; a and b) or fully deficient in *Bcl11b* (c–h). These chimeras were challenged with *N. brasiliensis* (a and b) or *C. rodentium* (c–h), and the indicated cell populations were enumerated by flow cytometry. (a and b) MLN ILC2 numbers (a) and intestinal worm burdens (b). Data represent two independent experiments with five to six mice per group; (a) mean ± SD; (b) mean ± SEM. (c and d) Weights after *C. rodentium* infection (single experiment with three mice per group; mean ± SD). (e) Bacterial load after *C. rodentium* infection (mean ± SEM). (f–h) Identification (f) and number (g) of ILC2 (lin$^-$CD45$^+$Id2-gfp$^+$IL7Rα$^+$KLRG1$^+$), ILC3 (lin$^-$CD45$^+$Id2-gfp$^+$IL7Rα$^+$NKp46$^+$ KLRG1$^-$; mean ± SD), and KLRG1$^{lo}$ cells (lin$^-$CD45$^+$Id2-gfp$^+$IL7Rα$^+$ NKp46$^+$KLRG1$^{lo}$) and intracellular staining of lineage$^-$ cells in the siLP (h) at day 26 p.i. with *C. rodentium*. (c and e–h) Data represent two independent experiments with eight to nine mice per group. P-values refer to Student's *t* test analysis: *, $P < 0.05$; **, $P < 0.01$; ***, $P < 0.001$.

*Rora*$^{sg/flox}$*Il7r*$^{Cre/+}$ BM plus *Bcl11b*$^{+/+}$*Id2*$^{gfp/+}$ FL rescued the ILC2-deficient phenotype caused by the production of ILC2s from the *Bcl11b*$^{+/+}$*Id2*$^{gfp/+}$ FL (Fig. 4 a), resulting in worm clearance similar to the control *Rora*$^{flox/+}$ mice (Fig. 4 b). Strikingly, *Bcl11b*$^{-/-}$*Id2*$^{gfp/+}$–derived FL reconstitution was unable to reverse the ILC2 deficiency (Fig. 4 a) and failed to efficiently clear *N. brasiliensis* by day 7 p.i. (Fig. 4 b). Thus, deletion of Bcl11b results in a critical loss of functional ILC2s, without which mice are unable to clear worm infection efficiently.

## Bcl11b deficiency does not impair ILC3 responses to *Citrobacter rodentium*

To investigate whether the absence of Bcl11b alters the functional capacity of ILC3s, we used the *C. rodentium* infection model. *C. rodentium* is a bacterial pathogen of mice that is closely related to the clinically important human enteropathogenic and enterohemorrhagic *E. coli*. Infection of wild-type mice with *C. rodentium* causes modest and transient weight loss and diarrhea, with clearance of infection within 21–28 d. In contrast, mice lacking ILC3s fail to control *C. rodentium* infection in the gut, as the result of insufficient IL-22 production, and succumb rapidly to infection (Satoh-Takayama et al.,

2008; Sonnenberg et al., 2011). Irradiated mice were reconstituted with either *Bcl11b*$^{+/+}$ or *Bcl11b*$^{-/-}$ FL before being challenged with *C. rodentium*. We observed no statistically significant differences in the weights of *Bcl11b*$^{+/+}$ or *Bcl11b*$^{-/-}$ FL reconstituted mice 20+ d p.i. (Fig. 4 c), contrasting markedly with the dramatic weight loss in *Rag2*$^{-/-}$γc$^{-/-}$ mice (Fig. 4 d). Both groups also cleared the majority of bacteria by day 21 p.i. (Fig. 4 e). Notably, the frequency of NCR$^+$ ILC3s was elevated in *C. rodentium*–infected *Bcl11b*$^{-/-}$ FL-reconstituted mice as compared with controls (Fig. 4, f–h), whereas ILC2s were absent. Bcl11b deficiency also resulted in the modest expansion of a KLRG1$^{lo}$NKp46$^+$ population, the etiology of which is unclear (Fig. 4 f). These results recapitulate the increase in NCR$^+$ ILC3 numbers we observed in naive Bcl11b-deficient mice.

The specific downstream gene targets of Bcl11b in ILC2s remain to be identified, and ChIP-Seq is challenging because of the small numbers of ILC2s available and uncertainty as to the exact sequence of the endogenous Bcl11b-binding site. However, studies of the T cell differentiation pathway suggest that Bcl11b can act as both a repressor and activator of transcription depending on its association with binding partners

(Liu et al., 2010) and on its state of phosphorylation or sumoylation (Avram and Califano, 2014).

It has been proposed that Bcl11b lies downstream of Notch signals that regulate its expression during T cell differentiation. We have reported previously that ILC2 development also requires Notch signals (Wong et al., 2012), and it is possible that these signals differentially regulate Bcl11b expression in ILC2s and T cells as compared with NK cells and ILC3s. Indeed, $Bcl11b^{-/-}$ DN2 thymocytes have been reported to express elevated levels of ILC3 and NK-inducing genes (including $Id2$, $Il2rb$, $Nfil3$, and $Plzf$), suggesting that these genes may be de-repressed in the absence of Bcl11b (Li et al., 2010a). However, it is not clear that a simple dominant master transcriptional regulator explains these differentiation pathways, and it is likely that the ILC and T cell transcription factor circuitry will share rheostats and resistors that are temporally and spatially regulated.

Collectively, these findings reveal a novel Bcl11b-mediated mechanism for the generation of ILC2s and demonstrate that this transcription factor is essential for ILC2 development and their functional role in helminth immunity. It is also noteworthy that mutations, duplications, and rearrangements in BCL11B are found in human hematological malignancies, including T cell acute lymphoblastic leukemia (T-ALL; Liu et al., 2010; Huang et al., 2012). The identification of a new role for Bcl11b in mouse ILC2 development raises the question of whether BCL11B acts in a similar way in human ILC2s and if the mutations in BCL11B may result in, as yet unidentified, ILC2 leukemia.

## MATERIALS AND METHODS

**Mice.** C57BL/6J, $Id2^{gfp/+}$ (Jackson et al., 2011), $Bcl11b^{tom/+}$ (Li et al., 2010b), $CreERT2;Bcl11b^{flox/-}$ (Li et al., 2010b), $IL7Rcre$ (Schlenner et al., 2010), $Rora^{flox/-}$ (Oliphant et al., 2014), B6SJL, and $Rag2^{-/-}\gamma c^{-/-}$ (Colucci et al., 1999) were all on a C57BL/6 background and bred in a specific pathogen–free facility. In individual experiments, all mice were matched for age, gender, and background strain. All animal experiments undertaken in this study were done so with the approval of the UK Home Office.

**Antibodies and flow cytometry.** Mouse tissue cell suspensions were incubated with purified anti-Fc receptor blocking antibody (anti-CD16/CD32) before addition of the specific antibodies. Cell surface markers were stained using a combination of FITC-, PE-, PE-Cy7–, PerCP-Cy5.5–conjugated, allophycocyanin-conjugated, Alexa Fluor 647–conjugated, eFluor 660–conjugated, eFluor 450–conjugated, Brilliant Violet 421–conjugated, Brilliant Violet 510–conjugated, Brilliant Violet 650–conjugated APC-Cy7–conjugated, and biotin-conjugated monoclonal antibodies. A cell viability marker was included to exclude dead cells from subsequent analysis. In each experiment, the appropriate isotype control monoclonal antibodies and single conjugate controls were also included. Samples were analyzed using an LSR Fortessa flow cytometer running FACSDiva acquisition (BD) and analyzed using FlowJo software (version 9.6.1; Tree Star). Cells were sorted using an iCyt Synergy cell sorter (Sony).

Antibodies for flow cytometry analysis included primary antibodies anti-CD4 (GK1.5), anti-CD8a (53-6.7), anti-CD19 (1D3), anti–Gr-1 (RB6-8C5), anti-CD11c (N418), anti-TER119 (TER-119), anti-CD25 (PC61.5), anti-CD44 (1M7), anti-CD45.1 (A20), anti-CD45.2 (104), anti-NK1.1 (PK136), anti-KLRG1 (2F1), fixable viability dye eFluor 780, and unconjugated anti-CD16/32 (93) and were purchased from eBioscience. Streptavidin conjugated to PE, PE-Cy7, or AF647 was purchased from eBioscience. Anti-ICOS

(C398.4A), anti-CD3e (145-2C11), anti-CD11b (M1/70), anti–IL-7Rα (SB/199), and anti-FcεRIα (MAR-1) were purchased from BioLegend. Anti-CD5 (53-7.3) was purchased from BD. Anti-T1/ST2 (DJ8) conjugated to biotin was purchased from MD Biosciences. All isotype control antibodies, rat anti–mouse IgG1, IgG2a, IgG2b, and Armenian hamster anti–mouse IgG were purchased from eBioscience.

**IL-25 and IL-33 administration.** rmIL-25 (0.5 µg per dose; Centocor) was administered daily for up to 4 d by intraperitoneal injection. rmIL-33 (0.5 µg per dose; BioLegend) was administered daily for 3 d by intraperitoneal injection or for 3 d (0.25 µg per dose) intranasally. Control mice received PBS only. Mice were euthanized 24 h after the final injection and tissues collected for analysis. Tamoxifen (1 mg per dose) was administered intraperitoneally in 100 µl vehicle, containing 90% sunflower oil (Sigma-Aldrich) and 10% ethanol. Conditional Bcl11b-deficient ($Bcl11b^{flox/-}$) mice were treated with six doses of tamoxifen and analyzed 3.5 wk later.

**OP9-DL1 cultures.** Cultures of ILC progenitor populations on OP9 and OP9-DL1 stroma (provided by J.C. Zúñiga-Pflücker, University of Toronto, Toronto, Ontario, Canada) were conducted as described previously (Wong et al., 2012).

**Adoptive cell transfer.** Putative ILC progenitor populations were FACS purified and collected into a 1:1 mixture of PBS and C57BL/6 mouse serum. Cells were injected directly into the tail vein of $Rag2^{-/-}\gamma c^{-/-}$ recipients (∼700 cells per recipient in a volume of 100 µl). Id2-gfp+ progeny were analyzed 3–6 wk after transfer.

**Irradiation chimeras.** Cell suspensions derived from embryonic day (E) 15.5 FLs were frozen in RPMI supplemented with 25% FCS and 10% DMSO and thawed immediately before reconstitution. For mixed chimera experiments, lethally irradiated C57BL/6 (CD45.2+) recipients were reconstituted with Bcl11b+/+ or Bcl11b−/− FL cells, either alone or as a 1:1 mixture (1–4 × 10⁶ cells) with BM derived from either B6SJL (CD45.1+) or $IL7Rcre; Rora^{flox/-}$ mice.

**Infection models.** For *N. brasiliensis* infection, mice were inoculated subcutaneously with 500 viable third-stage larvae and euthanized 4–7 d p.i. Tissues were collected for analysis, and small intestine worm burdens were enumerated using a dissection microscope (Wild M3Z; Leica). For *C. rodentium* infection, 100 ml LB broth containing 50 ng/ml nalidixic acid was inoculated with a single colony of *C. rodentium* (ICC180). Cultures were grown for 16 h at 37°C, with shaking, and then concentrated 10-fold in PBS. Mice were gavaged with 7 × 10⁹ CFU *C. rodentium* in 100 µl PBS. Weights of mice were recorded over the infection time course, and fecal pellets were collected at the indicated time points to ascertain the bacterial load. Pellets were weighed and resuspended in 100 µl PBS per 0.01 g. Supernatants from homogenized pellets were serially diluted and plated onto LB agar plates supplemented with 50 ng/ml kanamycin. Colonies were enumerated after overnight incubation at 37°C.

**Statistical analysis.** Prism (GraphPad Software) was used to calculate the SEM when different numbers of datasets existed in each experimental group. Statistical differences between groups were calculated using Student's *t* test, with $P < 0.05$ considered significant.

**Online supplemental material.** Flow cytometry gating strategies are described in Figs. S1–S3. Online supplemental material is available at http://www.jem.org/cgi/content/full/jem.20142224/DC1.

# JEM

## REFERENCES

Avram, D., and D. Califano. 2014. The multifaceted roles of Bcl11b in thymic and peripheral T cells: impact on immune diseases. *J. Immunol.* 193:2059–2065. http://dx.doi.org/10.4049/jimmunol.1400930

Barlow, J.L., R.J. Flynn, S.J. Ballantyne, and A.N. McKenzie. 2011. Reciprocal expression of IL-25 and IL-17A is important for allergic airways hyperreactivity. *Clin. Exp. Allergy.* 41:1447–1455. http://dx.doi.org/10.1111/j.1365-2222.2011.03806.x

Carotta, S., S.H. Pang, S.L. Nutt, and G.T. Belz. 2011. Identification of the earliest NK-cell precursor in the mouse BM. *Blood.* 117:5449–5452. http://dx.doi.org/10.1182/blood-2010-11-318956

Chang, Y.J., H.Y. Kim, L.A. Albacker, N. Baumgarth, A.N. McKenzie, D.E. Smith, R.H. Dekruyff, and D.T. Umetsu. 2011. Innate lymphoid cells mediate influenza-induced airway hyper-reactivity independently of adaptive immunity. *Nat. Immunol.* 12:631–638. http://dx.doi.org/10.1038/ni.2045

Colucci, F., C. Soudais, E. Rosmaraki, L. Vanes, V.L. Tybulewicz, and J.P. Di Santo. 1999. Dissecting NK cell development using a novel alymphoid mouse model: investigating the role of the c-abl proto-oncogene in murine NK cell differentiation. *J. Immunol.* 162:2761–2765.

Diefenbach, A., M. Colonna, and S. Koyasu. 2014. Development, differentiation, and diversity of innate lymphoid cells. *Immunity.* 41:354–365. http://dx.doi.org/10.1016/j.immuni.2014.09.005

Halim, T.Y., A. MacLaren, M.T. Romanish, M.J. Gold, K.M. McNagny, and F. Takei. 2012. Retinoic-acid-receptor-related orphan nuclear receptor alpha is required for natural helper cell development and allergic inflammation. *Immunity.* 37:463–474. http://dx.doi.org/10.1016/j.immuni.2012.06.012

Hams, E., R.M. Locksley, A.N. McKenzie, and P.G. Fallon. 2013. Cutting edge: IL-25 elicits innate lymphoid type 2 and type II NKT cells that regulate obesity in mice. *J. Immunol.* 191:5349–5353. http://dx.doi.org/10.4049/jimmunol.1301176

Hoyler, T., C.S. Klose, A. Souabni, A. Turqueti-Neves, D. Pfeifer, E.L. Rawlins, D. Voehringer, M. Busslinger, and A. Diefenbach. 2012. The transcription factor GATA-3 controls cell fate and maintenance of type 2 innate lymphoid cells. *Immunity.* 37:634–648. http://dx.doi.org/10.1016/j.immuni.2012.06.020

Huang, X., X. Du, and Y. Li. 2012. The role of BCL11B in hematological malignancy. *Exp. Hematol. Oncol.* 1:22. http://dx.doi.org/10.1186/2162-3619-1-22

Jackson, J.T., Y. Hu, R. Liu, F. Masson, A. D'Amico, S. Carotta, A. Xin, M.J. Camilleri, A.M. Mount, A. Kallies, et al. 2011. Id2 expression delineates differential checkpoints in the genetic program of CD8α^{+} and CD103^{+} dendritic cell lineages. *EMBO J.* 30:2690–2704. http://dx.doi.org/10.1038/emboj.2011.163

Li, L., M. Leid, and E.V. Rothenberg. 2010a. An early T cell lineage commitment checkpoint dependent on the transcription factor Bcl11b. *Science.* 329:89–93. http://dx.doi.org/10.1126/science.1188989

Li, P., S. Burke, J. Wang, X. Chen, M. Ortiz, S.C. Lee, D. Lu, L. Campos, D. Goulding, B.L. Ng, et al. 2010b. Reprogramming of T cells to natural killer–like cells upon *Bcl11b* deletion. *Science.* 329:85–89. http://dx.doi.org/10.1126/science.1188063

Liu, P., P. Li, and S. Burke. 2010. Critical roles of Bcl11b in T-cell development and maintenance of T-cell identity. *Immunol. Rev.* 238:138–149. http://dx.doi.org/10.1111/j.1600-065X.2010.00953.x

McKenzie, A.N., H. Spits, and G. Eberl. 2014. Innate lymphoid cells in inflammation and immunity. *Immunity.* 41:366–374. http://dx.doi.org/10.1016/j.immuni.2014.09.006

Mjösberg, J.M., S. Trifari, N.K. Crellin, C.P. Peters, C.M. van Drunen, B. Piet, W.J. Fokkens, T. Cupedo, and H. Spits. 2011. Human IL-25- and IL-33-responsive type 2 innate lymphoid cells are defined by expression of CRTH2 and CD161. *Nat. Immunol.* 12:1055–1062. http://dx.doi.org/10.1038/ni.2104

Molofsky, A.B., J.C. Nussbaum, H.E. Liang, S.J. Van Dyken, L.E. Cheng, A. Mohapatra, A. Chawla, and R.M. Locksley. 2013. Innate lymphoid type 2 cells sustain visceral adipose tissue eosinophils and alternatively activated macrophages. *J. Exp. Med.* 210:535–549. http://dx.doi.org/10.1084/jem.20121964

Moro, K., T. Yamada, M. Tanabe, T. Takeuchi, T. Ikawa, H. Kawamoto, J. Furusawa, M. Ohtani, H. Fujii, and S. Koyasu. 2010. Innate production of $T_H2$ cytokines by adipose tissue-associated c-Kit[+]Sca-1^{+} lymphoid cells. *Nature.* 463:540–544. http://dx.doi.org/10.1038/nature08636

Neill, D.R., S.H. Wong, A. Bellosi, R.J. Flynn, M. Daly, T.K. Langford, C. Bucks, C.M. Kane, P.G. Fallon, R. Pannell, et al. 2010. Nuocytes represent a new innate effector leukocyte that mediates type-2 immunity. *Nature.* 464:1367–1370. http://dx.doi.org/10.1038/nature08900

Oliphant, C.J., Y.Y. Hwang, J.A. Walker, M. Salimi, S.H. Wong, J.M. Brewer, A. Englezakis, J.L. Barlow, E. Hams, S.T. Scanlon, et al. 2014. MHCII-mediated dialog between group 2 innate lymphoid cells and CD4^{+} T cells potentiates type 2 immunity and promotes parasitic helminth expulsion. *Immunity.* 41:283–295. http://dx.doi.org/10.1016/j.immuni.2014.06.016

Price, A.E., H.E. Liang, B.M. Sullivan, R.L. Reinhardt, C.J. Eisley, D.J. Erle, and R.M. Locksley. 2010. Systemically dispersed innate IL-13–expressing cells in type 2 immunity. *Proc. Natl. Acad. Sci. USA.* 107:11489–11494. http://dx.doi.org/10.1073/pnas.1003988107

Satoh-Takayama, N., C.A. Vosshenrich, S. Lesjean-Pottier, S. Sawa, M. Lochner, F. Rattis, J.J. Mention, K. Thiam, N. Cerf-Bensussan, O. Mandelboim, et al. 2008. Microbial flora drives interleukin 22 production in intestinal NKp46^{+} cells that provide innate mucosal immune defense. *Immunity.* 29:958–970. http://dx.doi.org/10.1016/j.immuni.2008.11.001

Schlenner, S.M., V. Madan, K. Busch, A. Tietz, C. Läufle, C. Costa, C. Blum, H.J. Fehling, and H.R. Rodewald. 2010. Fate mapping reveals separate origins of T cells and myeloid lineages in the thymus. *Immunity.* 32:426–436. http://dx.doi.org/10.1016/j.immuni.2010.03.005

Sonnenberg, G.F., L.A. Monticelli, M.M. Elloso, L.A. Fouser, and D. Artis. 2011. CD4^{+} lymphoid tissue-inducer cells promote innate immunity in the gut. *Immunity.* 34:122–134. http://dx.doi.org/10.1016/j.immuni.2010.12.009

Stanya, K.J., D. Jacobi, S. Liu, P. Bhargava, L. Dai, M.R. Gangl, K. Inouye, J.L. Barlow, Y. Ji, J.P. Mizgerd, et al. 2013. Direct control of hepatic glucose production by interleukin-13 in mice. *J. Clin. Invest.* 123:261–271. http://dx.doi.org/10.1172/JCI64941

Wakabayashi, Y., H. Watanabe, J. Inoue, N. Takeda, J. Sakata, Y. Mishima, J. Hitomi, T. Yamamoto, M. Utsuyama, O. Niwa, et al. 2003. Bcl11b is required for differentiation and survival of αβ T lymphocytes. *Nat. Immunol.* 4:533–539. http://dx.doi.org/10.1038/ni927

Walker, J.A., J.L. Barlow, and A.N. McKenzie. 2013. Innate lymphoid cells—how did we miss them? *Nat. Rev. Immunol.* 13:75–87. http://dx.doi.org/10.1038/nri3349

Wong, S.H., J.A. Walker, H.E. Jolin, L.F. Drynan, E. Hams, A. Camelo, J.L. Barlow, D.R. Neill, V. Panova, U. Koch, et al. 2012. Transcription factor RORα is critical for nuocyte development. *Nat. Immunol.* 13:229–236. http://dx.doi.org/10.1038/ni.2208

Yagi, R., C. Zhong, D.L. Northrup, F. Yu, N. Bouladoux, S. Spencer, G. Hu, L. Barron, S. Sharma, T. Nakayama, et al. 2014. The transcription factor GATA3 is critical for the development of all IL-7Rα-expressing innate lymphoid cells. *Immunity.* 40:378–388. http://dx.doi.org/10.1016/j.immuni.2014.01.012